Observation of the Zero Hall Plateau in a Quantum Anomalous Hall Insulator

Yang Feng, Xiao Feng, Yunbo Ou, Jing Wang, Chang Liu, Liguo Zhang, Dongyang Zhao, Gaoyuan Jiang, Shou-Cheng Zhang, Ke He, Xucun Ma, Qi-Kun Xue, and Yayu Wang

Phys. Rev. Lett. **115**, 126801 — Published 16 September 2015

DOI: 10.1103/PhysRevLett.115.126801

Observation of the zero Hall plateau in a quantum anomalous Hall insulator

Yang Feng[1], Xiao Feng[1], Yunbo Ou[1,2], Jing Wang[3], Chang Liu[1], Liguo Zhang[1], Dongyang Zhao[1], Gaoyuan Jiang[1], Shou-Cheng Zhang[3,4], Ke He[1,4†], Xucun Ma[1,4], Qi-Kun Xue[1,4], Yayu Wang[1,4†]

[1]*State Key Laboratory of Low Dimensional Quantum Physics, Department of Physics, Tsinghua University, Beijing 100084, P. R. China*

[2]*Institute of Physics, Chinese Academy of Sciences, Beijing 100190, P. R. China*

[3]*Department of Physics, Stanford University, Stanford, CA 94305–4045, USA*

[4]*Collaborative Innovation Center of Quantum Matter, Beijing, China*

† Emails: kehe@tsinghua.edu.cn; yayuwang@tsinghua.edu.cn

We report experimental investigations on the quantum phase transition between the two opposite Hall plateaus of a quantum anomalous Hall insulator. We observe a well-defined plateau with zero Hall conductivity over a range of magnetic field around coercivity when the magnetization reverses. The features of the zero Hall plateau are shown to be closely related to that of the quantum anomalous Hall effect, but its temperature evolution exhibits significant difference from the network model for conventional quantum Hall plateau transition. We propose that the chiral edge states residing at the magnetic domain boundaries, which are unique to a quantum anomalous Hall insulator, are responsible for the novel features of the zero Hall plateau.

Quantum anomalous Hall (QAH) effect is a novel transport phenomenon in which the Hall resistance reaches the quantum plateau in the absence of an external magnetic field [1-3]. It represents an important member of the quantum Hall (QH) family, and may create unique applications in spintronic devices. The realization of this exotic effect requires that a two-dimensional (2D) material must be ferromagnetic (FM), topological, and insulating simultaneously [4]. Magnetically doped topological insulators (TIs) have been proposed to be an ideal material system for fulfilling these stringent requirements [1,2,5-7]. The inverted bulk band structure of a TI ensures topologically protected metallic surface states (SSs), which become 2D when the film is sufficiently thin [8]. The FM order induced by magnetic doping not only leads to the anomalous Hall effect, but also opens an energy gap at the Dirac point. When the Fermi level (E_F) is tuned into this gap, the only remaining conduction channel is the quasi-one-dimensional chiral edge state, which gives rise to quantized Hall resistance and vanishing longitudinal resistance at zero magnetic field [3,9].

Recently, the QAH effect has been observed experimentally in ultrathin films of magnetically doped Bi_2Te_3 family TI with accurately controlled chemical compositions grown by molecular beam epitaxy (MBE) [3,10-12]. It concludes a decade-long search for this exotic transport effect, and opens a new avenue for exploring the nature of the phases and phase transitions in topological quantum matters. An intriguing question concerning the QAH state is whether it is simply a zero-magnetic-field version of the QH effect, or if there is new physics beyond the conventional paradigm. An effective approach to address this issue is to investigate the quantum phase transition between the

two opposite Hall plateaus of a QAH insulator caused by magnetization reversal, and compare it with the plateau transitions in conventional QH effect.

In this letter we report transport studies on a QAH insulator with relatively high magnetic doping level. We observe a well-defined plateau with zero Hall conductivity over a range of magnetic field around coercivity, consistent with a recent theoretical prediction [13]. The features of the zero Hall plateau are shown to be related to that of the QAH effect, but its temperature evolution exhibits significant difference from the network model for conventional QH plateau transition [14]. We propose that the chiral edge states residing at the magnetic domain boundaries, which are unique to a QAH insulator, are responsible for the novel features of the zero Hall plateau. The rich magnetic domain structure and dynamics make the QAH effect a distinctive class of quantum phenomenon that may find unique applications in spintronics.

The MBE-grown QAH insulator thin film studied here has a chemical formula $Cr_{0.23}(Bi_{0.4}Sb_{0.6})_{1.77}Te_3$ and thickness d = 5 QL (quintuple layer). The sample growth and transport measurement methods are similar to that reported previously [3]. Shown in Fig. 1(a) is a schematic drawing of the transport device. The film is manually scratched into a Hall bar geometry, and the $SrTiO_3$ substrate is used as the bottom gate oxide due to its large dielectric constant at low temperature. The Cr concentration, hence the density of local moment, is higher than that in the sample where the QAH effect was originally discovered [3]. As a result, the FM order forms at a higher Curie temperature T_C = 24 K as determined by the temperature dependent anomalous Hall effect (supplementary Fig. S1 [15][16]). Another consequence of higher Cr doping is at the microscopic scale the

sample becomes more disordered (although it remains uniform macroscopically, see Fig. S2), which is crucial to the physics that will be discussed in this work.

We first demonstrate the existence of QAH effect in this sample. Fig. 1(b) displays the gate voltage (V_g) dependence of the Hall resistance ρ_{yx} (blue curve) and longitudinal resistance ρ_{xx} (red curve) measured at T = 10 mK in a strong magnetic field B = 12 T applied perpendicular to the film. The ρ_{yx} exhibits a plateau for -10 V < V_g < 10 V with its maximum value close to 99.1% of the quantum resistance h/e^2 ~ 25.8 kΩ. In the same V_g range ρ_{xx} shows a pronounced dip with its minimum value close to 0.1 h/e^2. In Fig. 1(c) we display the field dependence of ρ_{yx} measured at V_g = -5 V, when ρ_{xx} reaches a minimum in Fig. 1(b). The Hall trace shows an abrupt jump at zero magnetic field, characteristic of the anomalous Hall effect. With increasing magnetic field, the ρ_{yx} value increases gradually and approaches h/e^2 at 12 T. The ρ_{xx} shown in Fig. 1(d) exhibits two sharp peaks at the coercive field H_C, and decreases rapidly on both sides. The ρ_{xx} value is around 3 h/e^2 at zero field, but is significantly suppressed to 0.1 h/e^2 at $\mu_0 H$ = 12 T. The overall trend is the same as that shown in the original report of QAH effect [3].

To reveal the nature of the quantum phase transition between the two opposite QAH plateaus, in Figs. 2(a) and 2(b) we zoom into the low field part of the curves in Fig. 1(c) and 1d. Although the ρ_{yx} curve [Fig. 2(a)] shows the typical square-shaped hysteresis, the zero field ρ_{yx} value is around 0.9 h/e^2 and the transition near H_C is rather smooth. In the butterfly-shaped ρ_{xx} curve [Fig. 2(b)], the peak ρ_{xx} value at H_C reaches 35 h/e^2, much larger than that reported previously [3]. Both observations can be explained by the high degree of disorder and small domain size in the current sample with larger Cr

concentration, which is not ideal for the achievement of QAH effect. A highly intriguing phenomenon can be revealed when we convert the measured resistivity to longitudinal and Hall conductivity σ_{xx} and σ_{xy} by using the tensor relation:

$$\sigma_{xx} = \frac{\rho_{xx}}{\rho_{xx}^2+\rho_{yx}^2} \text{ and } \sigma_{xy} = \frac{\rho_{yx}}{\rho_{xx}^2+\rho_{yx}^2}.$$

Fig. 2(c) displays the σ_{xx} and σ_{xy} converted from the resistivity data shown in Fig. 2(a) and 2b. At H_C = 0.16 T, the longitudinal conductivity (red curve) shows a minimum with σ_{xx} ~ 0.03 e^2/h, reflecting the highly insulating behavior when the magnetic domains reverse. The Hall conductivity (blue curve), interestingly, shows a plateau with σ_{xy} = 0 spanning a field scale of ~0.12 T centered around H_C. This zero Hall plateau, which was theoretically predicted in Ref. 7, has never been observed before by experiment and is the main focus of the current work.

To unveil the origin of the zero Hall plateau, in Fig. 3 we display the magnetic field dependent σ_{xy} curves measured under varied gate voltages at T = 50 mK (raw data of ρ_{xx} and ρ_{yx} are displayed in Fig. S3). For V_g between -10 V and +10 V [Fig. 3(b)-(f)], there is always a well-defined zero Hall plateau around H_C. This gate voltage range corresponds to the QAH plateau in Fig. 1(b), when E_F lies within the magnetic gap at the Dirac point. When the V_g value is increased to ±30 V [Fig. 3(a) and 3(g)], which are outside the QAH regime, the zero Hall plateau feature is much weakened and the Hall conductivity merely shows a shoulder-like curvature around H_C. This gate voltage dependence clearly indicates that the zero Hall plateau is closely related to the QAH effect.

The same conclusion can be drawn from the temperature evolution of the zero Hall plateau. Shown in Fig. 4(a) and 4(b) are the conductivity measured at seven different

temperatures under a fixed V_g = -5 V (the raw data of ρ_{xx} and ρ_{yx} are displayed in Fig. S4). The σ_{xx} curves in Fig. 4(a) show that with increasing temperature, the H_C decreases and the minimum σ_{xx} value at H_C increases. This is due to the increase of thermally activated parallel SS conduction at higher temperatures. The σ_{xy} curves in Fig. 4(b) show that the zero Hall plateau near H_C narrows at high temperatures, and becomes barely visible at T = 3 K. This is accompanied by the decreases of high field σ_{yx} value due to the weakening of QAH effect at high temperatures. In Fig. 4(c) we plot the temperature dependence of the zero Hall plateau width and the ρ_{yx} value at 12 T extracted from Fig. S4. The two quantities closely track each other, again demonstrating the intimate correlation between the zero Hall plateau and the QAH effect.

Both the gate voltage and temperature dependence indicate that the zero Hall plateau originates from the same physical mechanism as the QAH effect, namely the quantum transport by the spontaneously generated chiral edge states. The difference is that in the QAH regime, all the magnetic domains in the FM TI are aligned along the same direction, thus there is only one pair of chiral edge states propagating along the sample boundary [6]. The zero Hall plateau, on the contrary, occurs around the coercive field when the magnetic domains reverse. Near H_C there are a large number of randomly distributed upward and downward domains, leading to the proliferation of chiral edge states at the domain walls. The phenomenology of the zero Hall plateau should be explained by considering the transport properties of this network of chiral edge states.

Recently, a microscopic model has been proposed to describe the critical properties of the plateau transition in a QAH insulator [13]. The basic physical picture is that at the coercive field, the chiral edge states at the magnetic domain walls may tunnel into each

other when the distance between them is shorter than the spatial decay length of the edge state. Therefore, the plateau transition at the coercivity in a QAH insulator can be mapped to the network model of the integer QH plateau transition in the lowest Landau level (LL) [14,17-19]. It was predicted that an intermediate plateau with zero Hall conductivity could occur at H_C, and the longitudinal conductivity will show two peaks [13]. The mechanism for the zero Hall plateau is that during magnetization reversal near H_C, the mean value of the exchange field gap induced by FM order approaches 0. Accordingly, the system is transitioned into an insulating state where the first Chern number becomes $C_1 = 0$ and $\sigma_{xy} = C_1 \cdot e^2/h = 0$.

Although the zero Hall plateau feature observed here is qualitatively consistent with the theoretical prediction in Ref. 7, a closer examination of the data reveals quantitative differences. First, the σ_{xx} curves shown in Fig. 4(a) reach a minimum at H_C and increase monotonically on both sides. This is inconsistent with the double-peak structure predicted in the theory [13]. More importantly, the temperature evolution of the σ_{xy} curves shown in Fig. 4(b) cannot be described by the scaling law laid out in the theory [20,21]. The blue open circles in Fig. 4(d) depict the temperature dependence of the slope of the σ_{xy} vs. H curve just outside the zero Hall plateau. It decreases gradually with lowing T, and becomes almost a constant below T = 200 mK. This is opposite to the theoretical prediction of the divergence of the slope as T decreases towards zero [13].

One reason for the inconsistency between theory and experiment is the sample studied here is not as perfect as considered theoretically due to the residual SS conduction. For a more ideal QAH insulator (Fig. S5a), the σ_{xx} curve indeed shows a weak but visible double-peak structure (Fig. S5b upper panel). However, in such a sample the zero Hall

plateau in σ_{xy} is much weakened, only showing a slight curvature near H_C (Fig. S5b lower panel). This is because the occurrence of zero Hall plateau requires the sample to break up into many small magnetic domains at H_C to create a large number of chiral edge states at domain walls. The current sample with high Cr doping and strong disorder favors the domain proliferation, but an ideal QAH sample with weak disorder prefers the formation of a small number of large domains during magnetization reversal. This picture is further confirmed by the Cr doping dependent results shown in Fig. S6, where the QAH plateau becomes less perfect with increasing Cr content, but the zero Hall plateau becomes more pronounced (as indicated by the plateau width in Fig. S7).

The temperature dependence of the slope of σ_{xy} shown in Fig. 4(d) is more puzzling. In the network model for conventional QH effect, the plateau transition becomes steeper at lower temperature due to the increase of phase coherence length [22-24]. We propose that the most likely cause of the anomalous behavior here is due to the magnetic domain dynamics in a QAH insulator. For a FM material, the shape of the magnetic hysteresis loop is a very complicated issue that depends on various factors including magnetic anisotropy, strength of the exchange coupling and homogeneity of the sample [2,25]. In the current sample, the steeper slope of σ_{xy} at higher temperature indicates that the reversal of magnetic domain becomes easier with increasing T, although its exact reason is unclear at the moment. The dominant factor here is thus not the phase coherence length of the edge states, but instead the peculiar magnetic domain dynamics or domain structure (such as canted magnetization) of the FM TI. Although such physics is not included in the network model for the QH plateau transition, the very existence of the

chiral edge states at the domain boundaries is a robust feature of the QAH state and is insensitive to the details of the domain structure.

The zero Hall plateau state discovered here is absent in ordinary 2D electron systems with parabolic dispersion because no zeroth LL is allowed. Even for 2D Dirac fermion system with zeroth LL, the observed zero Hall plateau [26,27] is microscopically different from the multi-domain network of chiral edge states discussed above. For example, the diverging ρ_{xx} at the zero-energy state in graphene QH state is found to have a field-induced metal-insulator transition with Kosterlitz-Thouless type [28]. Whereas for the zero Hall plateau state here, the T dependence of the peak ρ_{xx} value at H_C exhibits a more complex behavior. As shown in Fig. 4(d), for temperatures above 200 mK the peak ρ_{xx} value can be fit very well by using the variable range hopping formula. The physical mechanism is also related to the magnetization reversal at the coercivity of a QAH insulator, when the electrical conduction is contributed from the tunneling between the chiral edge states residing on the magnetic domain boundaries. Because of the random distribution of the domains hence the edge states, the conduction process is very similar to the variable range hopping of electrons in disordered electronic systems. The hopping is strongly suppressed with decreasing temperature, leading to the rapid increase of resistivity. The deviation from the variable range hopping fit below 200 mK suggests that the sample enters a new insulating ground state whose nature is still unknown.

In summary, we observe a zero Hall plateau at the coercivity of a QAH insulator. From the quantum phase transition perspective, the QAH effect may not be a simple zero-field version of the QH effect due to the unique domain wall dynamics. A new theoretical model is required to describe the scaling behavior and critical properties of the

QAH plateau transition, which is manifested by the zero Hall plateau. From the application point of view, in recent years there are significant progresses in utilizing the nano-sized domains in FM materials for achieving new spintronic devices, such as the race track memory [29]. The quantum transport properties of the chiral edge states, in conjunction with the rich magnetic domain dynamics of a QAH insulator, may give rise to novel spintronic properties. For example, the zero Hall plateau state has been proposed to host quantized topological magneto-electric effect [30], and observing this effect is the subject of ongoing work.

Reference:

[1] C. X. Liu, X. L. Qi, X. Dai, Z. Fang, and S. C. Zhang, Phys. Rev. Lett. **101**, 146802 (2008).

[2] R. Yu, W. Zhang, H. J. Zhang, S. C. Zhang, X. Dai, and Z. Fang, Science **329**, 61 (2010).

[3] C.-Z. Chang *et al.*, Science **340**, 167 (2013).

[4] K. He, X. C. Ma, X. Chen, L. Lu, Y. Y. Wang, and Q. K. Xue, Chin. Phys. B **22**, 067305 (2013).

[5] X. L. Qi, Y. S. Wu, and S. C. Zhang, Phys. Rev. B **74**, 085308 (2006).

[6] X. L. Qi, T. L. Hughes, and S. C. Zhang, Phys. Rev. B **78**, 195424 (2008).

[7] K. Nomura and N. Nagaosa, Phys. Rev. Lett. **106**, 166802 (2011).

[8] Y. Zhang *et al.*, Nat. Phys. **6**, 584 (2010).

[9] J. Wang, B. Lian, H. J. Zhang, and S. C. Zhang, Phys. Rev. Lett. **111**, 086803 (2013).

[10] J. G. Checkelsky, R. Yoshimi, A. Tsukazaki, K. S. Takahashi, Y. Kozuka, J. Falson, M. Kawasaki, and Y. Tokura, Nat. Phys. **10**, 731 (2014).

[11] X. F. Kou *et al.*, Phys. Rev. Lett. **113**, 137201 (2014).

[12] C.-Z. Chang *et al.*, Nat Mater **advance online publication** (2015).

[13] J. Wang, B. Lian, and S. C. Zhang, Phys. Rev. B **89**, 085106 (2014).

[14] B. Kramer, T. Ohtsuki, and S. Kettemann, Phys. Rep. **417**, 211 (2005).

[15] A. Arrott, Phys. Rev. **108**, 1394 (1957).

[16] See Supplemental Material [url], which includes Refs. [3,13,15].

[17] S. Kivelson, D. H. Lee, and S. C. Zhang, Phys. Rev. B **46**, 2223 (1992).

[18] B. Huckestein, Rev. Mod. Phys. **67**, 357 (1995).

[19] S. L. Sondhi, S. M. Girvin, J. P. Carini, and D. Shahar, Rev. Mod. Phys. **69**, 315 (1997).

[20] E. Abrahams, P. W. Anderson, P. A. Lee, and T. V. Ramakrishnan, Phys. Rev. B **24**, 6783 (1981).

[21] W. L. Li, C. L. Vicente, J. S. Xia, W. Pan, D. C. Tsui, L. N. Pfeiffer, and K. W. West, Phys. Rev. Lett. **102**, 216801 (2009).

[22] A. M. M. Pruisken, Phys. Rev. Lett. **61**, 1297 (1988).

[23] B. Huckestein and B. Kramer, Phys. Rev. Lett. **64**, 1437 (1990).

[24] Y. Huo and R. N. Bhatt, Phys. Rev. Lett. **68**, 1375 (1992).

[25] Z. Ge and U. o. N. Dame, *Magneto-transport Studies of Ferromagnetic (gallium,manganese)arsenide Heterostructures* (University of Notre Dame, 2008).

[26] Y. Zhang *et al.*, Phys. Rev. Lett. **96**, 136806 (2006).

[27] Y. Zhao, P. Cadden-Zimansky, Z. Jiang, and P. Kim, Phys. Rev. Lett. **104**, 066801 (2010).

[28] J. G. Checkelsky, L. Li, and N. P. Ong, Phys. Rev. Lett. **100**, 206801 (2008).

[29] S. S. P. Parkin, M. Hayashi, and L. Thomas, Science **320**, 190 (2008).

[30] J. Wang, B. Lian, X.-L. Qi, and S.-C. Zhang, arXiv preprint arXiv:1506.03141 (2015).

Acknowledgements

Y.F. and X.F. contributed equally to this work. This work was supported by the National Natural Science Foundation of China and the Ministry of Science and Technology of China. J. W. and S.C. Z. acknowledge the support from the U.S. Department of Energy, Office of Basic Energy Sciences, Division of Materials Sciences and Engineering, under contract No. DE-AC02-76SF00515, and from the FAME Center, one of six centers of STARnet, a Semiconductor Research Corporation program sponsored by MARCO and DARPA.

Figure captions:

FIG. 1 (color online). (a) Schematic drawing of the transport device used in this study. (b) Gate voltage V_g dependence of ρ_{yx} (blue curve) and ρ_{xx} (red curve) measured at T = 10 mK in a B = 12 T. (c) and (d) Magnetic field dependence of ρ_{yx} (blue curve) (c) and ρ_{xx} (red curve) (d) measured at T = 50 mK and V_g = -5 V.

FIG. 2 (color online). Low field part of the hysteretic anomalous Hall curve (blue curve) (a) and butterfly-shaped magnetoresistance (red curve) (b) measured at T = 50 mK and V_g = -5 V. (c) Magnetic field dependence of σ_{xx} (red curve) and σ_{xy} (blue curve), showing a minimum of $\sigma_{xx} \sim 0.03\ e^2/h$ and a Hall plateau with $\sigma_{xy} = 0$ around H_C = 0.16 T.

FIG. 3 (color online). (a) to (g): The σ_{xy} for various V_g values at -30 V, -10 V, -5 V, 0 V, +5 V, +10 V and +30 V, respectively. The zero Hall plateau clearly exists for V_g between -10 V and +10 V and becomes weakened when V_g value is increased to ± 30 V.

FIG. 4 (color online). The σ_{xx} (a) and σ_{xy} (b) measured at seven different temperatures at V_g = -5 V. (c) Close correlation between the temperature dependences of zero Hall plateau width and ρ_{yx} value at 12 T. (d) Dependence of the peak ρ_{xx} value at H_C (black open squares) and the maximum slope of σ_{xy} vs. $\mu_0 H$ curve near H_C (blue open circles). The dashed red line shows the variable range hopping fit between 200 mK to and 3 K. Note both the x and y axes are in logarithmic scale.

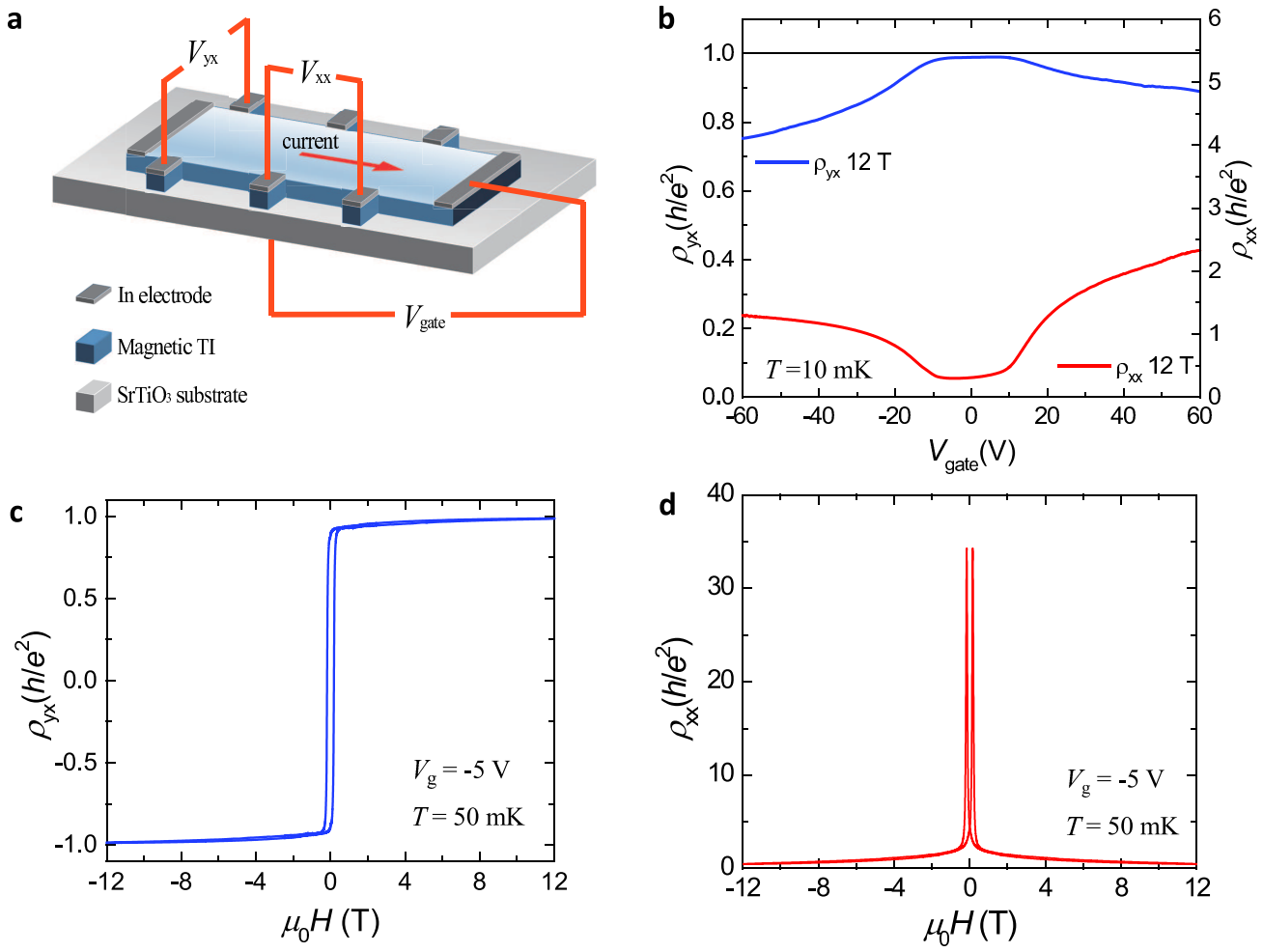

Figure 1 LC15720 21AUG2015

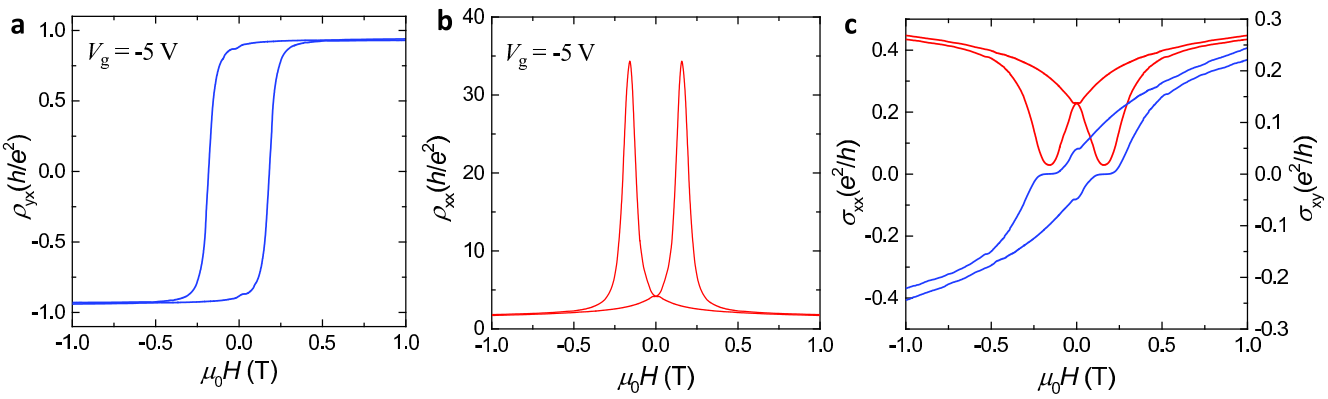

Figure 2 LC15720 21AUG2015

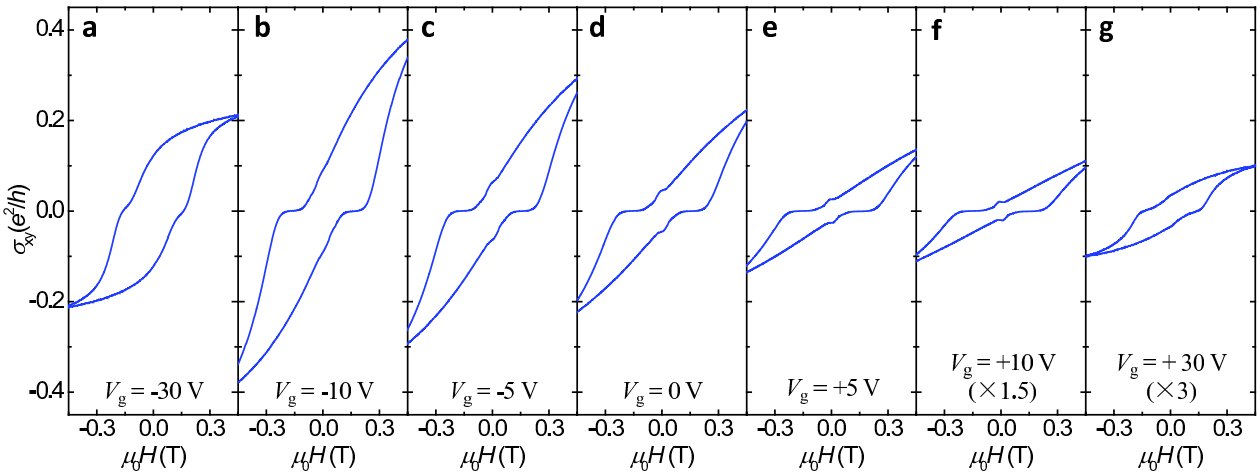

Figure 3 LC15720 21AUG2015

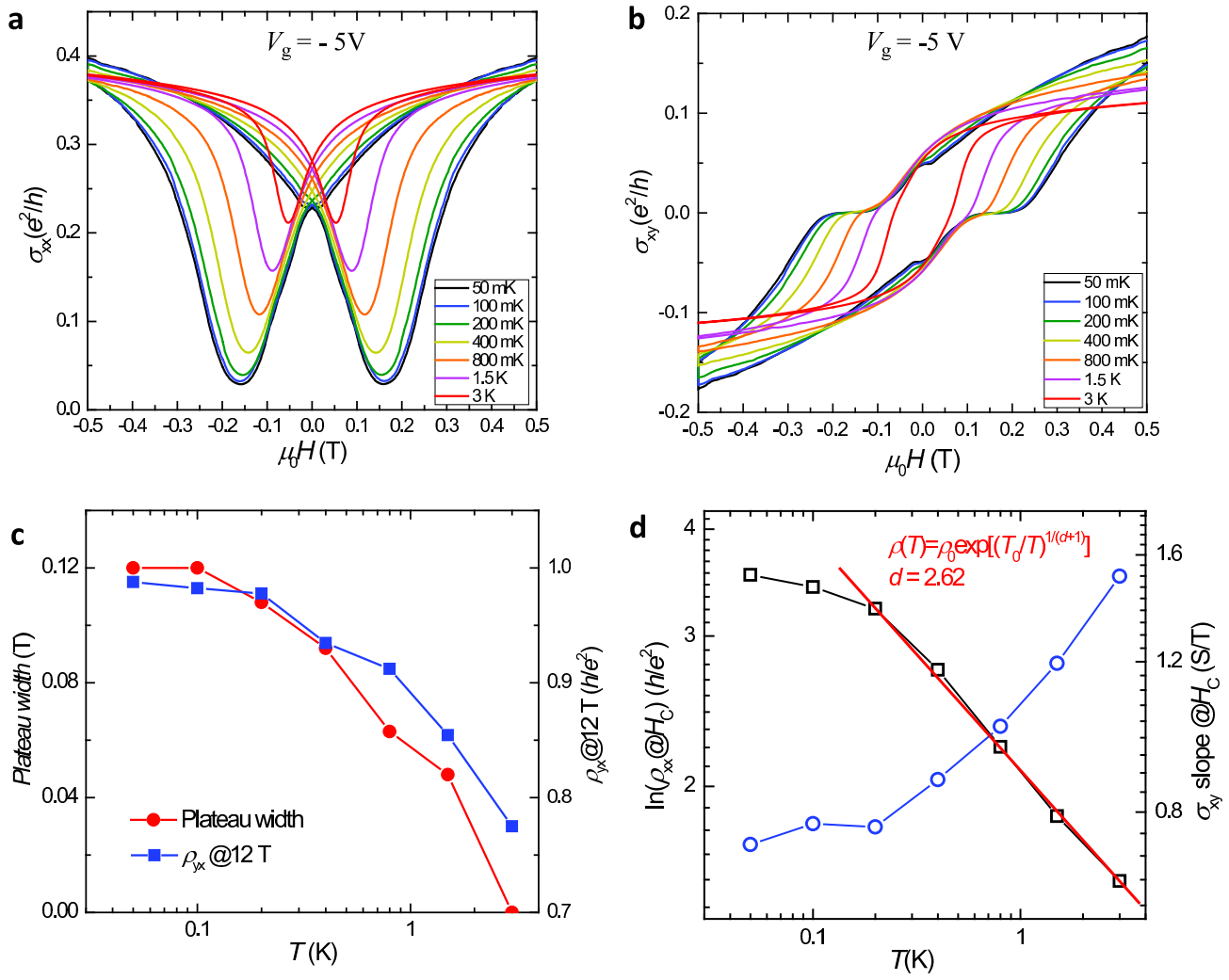

Figure 4 LC15720 21AUG2015